

Effects of Real Airfoil Geometry on Leading Edge Gust Interaction Noise

James Gill*, Xin Zhang†, and Phillip Joseph‡

*Faculty of Engineering and the Environment,
University of Southampton, Hampshire, SO17 1BJ, UK.*

Thomas Node-Langlois§,

*Acoustics and Environment - Numerical Methods,
Airbus Operations S.A.S, 31060 Toulouse, France.*

High-order computational aeroacoustic methods are applied to the modeling of noise due to interactions between gusts and the leading edge of real symmetric airfoils. The effects of airfoil thickness and leading edge radius on noise are investigated systematically and independently for the first time, at higher frequencies than previously used in computational methods. Single frequency harmonic gusts are interacted with airfoils of varying geometry at zero angle of attack. Increases in both leading edge radius and thickness are found to reduce the predicted noise. This noise reduction effect becomes greater with increasing frequency and Mach number. The dominant noise reduction mechanism for airfoils with real geometry is found to be related to the leading edge stagnation region. The assumption of uniform meanflow is shown to be invalid when modeling the leading edge noise of real airfoils. However, accurate results are still obtained when an inviscid meanflow is assumed. The accuracy of analytic flat plate solutions can be expected to decrease with increasing airfoil thickness, leading edge radius, gust frequency and Mach number.

Keywords: computational aeroacoustics, gust response, leading edge noise, linearized Euler equations

Nomenclature

λ	Vortical gust wavelength	m	U_x	Freestream velocity	ms^{-1}
θ	Observer angle	deg	w	Instantaneous gust velocity	ms^{-1}
			w_0	Maximum gust velocity	ms^{-1}
c	Airfoil chord	m	x	Streamwise location	m
I	Leading edge shape parameter				
K	Chord-based reduced frequency	$K = c/\lambda$			
k_g	Vortical gust wavenumber	m^{-1}	CAA	Computational AeroAcoustics	
K_t	Thickness-based reduced frequency	$K_t = t/\lambda$	CROR	Contra-Rotating Open Rotor	
n	Number of discrete gusts		FW-H	Ffowcs-Williams and Hawkings	
R_{le}	Leading edge radius	m	LEE	Linearized Euler Equations	
T	Time	s	PWL	sound PoWer Level	dB
t	Maximum airfoil thickness	m	SPL	Sound Pressure Level	dB

*EngD student, Aeronautics Astronautics and Computational Engineering, J.Gill@soton.ac.uk.
†Airbus Professor of Aircraft Engineering, Aeronautics Astronautics and Computational Engineering, Associated fellow, AIAA.
‡Professor of Engineering Acoustics, ISVR.
§Acoustic engineer, Acoustics and Environment Department, Airbus.

I. Introduction

THE noise produced by interactions between an oncoming unsteady vortical gust and the leading edge of an airfoil has been of interest for many years. It is a significant contributor to the noise in turbo-machinery for example. Additionally this noise generation mechanism has received renewed interest in relation to contra rotating open rotor engines (CRORs) because they have potential to help meet EU Flightpath 2050 targets, which call for 75%, 90%, and 65% reductions in CO_2 , NO_x , and noise emissions respectively, against 2000 baselines¹.

A significant body of work exists on the subject of predicting leading edge gust interaction noise using analytical approaches. The early work by Sears² (who derived a model to predict the unsteady lift and moment from a flat plate encountering a sinusoidal gust in incompressible flow) has been extended to compressible flow problems by Graham³ and Amiet⁴. Amiet⁴ used this theory to predict leading edge noise emissions from an isolated flat plate interacting with oncoming turbulence. Models that are used to predict broadband leading edge noise in CROR engines (and to predict broadband rotor-stator interaction noise in turbofans) are often still based on Amiet's flat plate model. However, the effects of real airfoil geometry on leading edge gust interaction noise have not been fully addressed.

Previous studies (which are discussed in Section II) have used a variety of experimental, computational aeroacoustic (CAA), and analytic methods to investigate the implications of assuming a flat plate geometry as opposed to modeling a realistic airfoil shape, but these studies have not found a consensus on all aspects. This paper applies CAA methods to systematically explore the effects of real airfoil geometry on leading edge gust interaction noise. It also provides a measure of the validity of analytic flat plate models when they are used to predict the leading edge noise from real airfoils.

If the geometry of an airfoil is changed, then the flow surrounding the airfoil will also be altered. The steady meanflow surrounding a flat plate can be assumed to be uniform (i.e. $U(x, y) = U_x$, where $U(x, y)$ and U_x are the local and freestream velocities respectively). However, for real airfoils the steady meanflow is non-uniform, and the asymptotic nature of flow features such as the leading edge stagnation region can be difficult to include in analytic models. Therefore, if the implications on noise predictions are small, complex analytical modeling of non-uniform flow around an airfoil may be avoided by also assuming $U(x, y) = U_x$ for airfoils with real geometry. The current work aims to investigate the validity of simplifying the modeling of the meanflow when making leading edge noise predictions for real airfoils. To the authors' knowledge, The effects of a simplified meanflow modeling approach for leading edge noise have not previously been investigated.

By using a CAA code which solves the linearized Euler equations (LEE) to describe the unsteady flow about symmetric real airfoils, this work addresses the following:

- The effects of thickness and leading edge radius on the noise due to symmetric airfoils at varying Mach number, for single frequency harmonic vortical gusts convecting with a steady meanflow. The noise is studied at reduced frequencies which are higher than previously tested in computational studies.
- The effects on noise predictions when simplifying assumptions are made concerning the steady meanflow surrounding an airfoil. The validity of assuming a uniform meanflow or an inviscid meanflow is assessed.
- The underlying mechanism which causes changes in the noise due to real airfoils interacting with vortical gusts, compared to predictions made with flat plate theory.

A schematic of a single harmonic vortical gust interacting with a symmetric airfoil is shown in Figure 1.

II. Previous work

Previous studies have investigated the effect of real airfoil geometry on the noise due to unsteady vortical disturbances impinging on an airfoil leading edge. These have included analytic, experimental, and CAA approaches, and have concentrated on the effects on noise due to airfoil thickness, angle of attack, and camber. Previous work has not considered the effects on noise due to the leading edge radius, which is an additional length-scale considered in this paper.

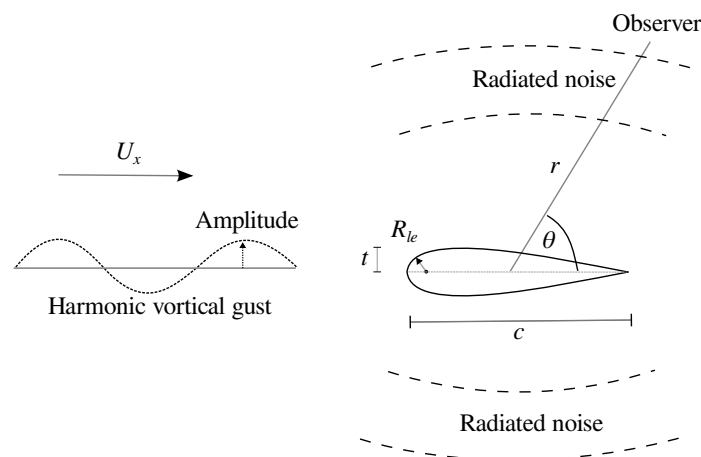


Figure 1. A schematic of a single frequency harmonic gust interacting with an airfoil at zero angle of attack, where t is the airfoil thickness, R_{le} is the leading edge radius, c is the airfoil chord, U_x is the freestream velocity, r is the observer radius and θ is the observer angle from the downstream direction.

II.A. Effects of angle of attack and camber

Flat plate theory is restricted to studying the interactions between gusts and flat plates at zero angle of attack. The effect of this angle of attack limitation on noise has been experimentally investigated by authors such as Staubs,⁵ Devenport et al.⁶ and Paterson and Amiet⁷, and has been concluded to be small for reduced frequencies up to $K = 6.7$. In addition to studying angle of attack effects, Devenport et al. also considered the effect of camber (which is also not modeled by flat plate theory) and found it to have a small effect on the noise, similar in magnitude to the effect of angle of attack. Because the effects of airfoil camber and angle of attack on noise predictions are expected to be small, these aspects of airfoil geometry are not considered in this paper.

II.B. Effects of thickness

The effect of airfoil thickness on leading edge noise has received considerable attention from previous authors because it has a more significant effect on noise than camber or angle of attack.

II.B.1. Experimental studies

Paterson and Amiet⁷ measured the noise due to an isolated NACA 0012 airfoil interacting with nearly isotropic grid-generated turbulence at speeds of up to 165 ms^{-1} . The paper was the first to note that airfoil thickness reduces the noise compared to flat plate predictions, with the effect being more pronounced at high frequencies. A 5 dB reduction in noise was measured from the NACA 0012 airfoil compared with analytic flat plate solutions. The 5 dB reduction in noise due to the thickness of the NACA 0012 airfoil was measured at a thickness-based reduced frequency $K_t = t/\lambda = 1$ (where t is airfoil thickness and λ is the vortical gust wavelength). This frequency was suggested by Paterson and Amiet as a measure of when flat plate theory breaks down and can no longer be considered accurate. Further experimental studies by authors such as Olsen and Wagner⁸, and Devenport et al.⁶ measured the leading edge noise from airfoils with differing thicknesses, and reported that the noise is reduced as airfoil thickness and the gust frequency is increased.

II.B.2. Analytic studies

Most analytic models for the prediction of leading edge gust interaction noise are restricted to flat plates. However, there have been some attempts at extending the theory to include real geometry effects. Glegg and Devenport⁹ showed with a conformal mapping approach that the effect of increasing thickness is to reduce the noise at high frequencies. Moreau et al.¹⁰ modified existing flat plate analytic theory with semi-empirical corrections, based on observations of thickness effects in experimental studies. Chiang and Fleeter¹¹ analytically found that increasing the airfoil thickness has the effect of reducing the leading edge

noise, because the amplitude of the leading edge surface pressure response is reduced and smoothed over a larger section of the airfoil chord.

II.B.3. Computational studies

Compared to experimental and analytic studies, there are relatively few CAA studies which investigate the effects of airfoil geometry on leading edge noise. Furthermore, these studies have been restricted to modeling a small number of discrete frequencies, using single frequency harmonic gusts. The use of single frequency harmonic gusts means that any effects of turbulence length-scale are neglected, as well as the effects from gusts whose wavefront is not normal to the meanflow direction. Evers and Peake¹² have shown with an analytic model to predict cascade noise that the leading edge noise due to turbulent flow exhibits a weaker sensitivity to airfoil geometry than flow containing harmonic disturbances. However, the use of harmonic disturbances is still useful in revealing general trends between the leading edge noise and changes in airfoil geometry.

Atassi et al.¹³ investigated the effects of thickness on the noise due to a harmonic gust by using a CAA method which solved the 2D linearized Euler equations in the frequency domain. They investigated Joukowski airfoils with thicknesses ranging from 3% to 12% of the airfoil chord, and found that in $M = 0.5$ flow at reduced frequencies of $K = c/\lambda \sim 1$ or higher, the effect of thickness was to reduce the noise at downstream observer locations, and increase it at upstream locations. Therefore, the basic shape of the directivity was unaltered, but the resulting pattern was skewed towards the upstream direction when compared with flat plate predictions. It was also observed that the thickness effect is more pronounced at higher freestream Mach numbers.

Lockard and Morris¹⁴ performed a CAA study of noise radiated by NACA 4-series airfoils encountering harmonic vortical gusts in the time domain. They used both inviscid Euler and viscous Navier-Stokes calculations to model vortical gust interactions up to $K \sim 1.2$ in $M = 0.5$ flow. Lockard and Morris made similar conclusions to Atassi et al., where airfoil thickness caused an upstream skewing of the directivity pattern such that the noise was reduced at downstream observer locations by a greater amount than at upstream locations. Lockard and Morris gave the realistic airfoil curvature and the realistic meanflow solution as the dominant causes for the change in the noise.

II.B.4. Summary

In the previous work described above, there is clearly some agreement between the conclusions from each study as to the effects on noise due to airfoil thickness. All studies have found that the noise is reduced significantly at high frequency due to increasing airfoil thickness. However, the computational studies found a forward skewing of the directivity pattern with increasing thickness, whereas experimental noise measurements did not show this behavior. Additionally, Paterson and Amiet⁷ suggested that flat plate theory is inaccurate for 12% thick airfoils at reduced frequencies above $K_t = 1$ (or $K = 8.3$ for 12% thick airfoils), whereas Atassi et al.¹³ reported that thickness effects on noise become apparent for $K > 1$.

One reason why experimental measurements have not found an upstream skewing of the directivity pattern may be because the wind tunnel nozzle can prevent adequate microphone placement at acute upstream observer positions. Because of this, the experimental studies discussed here limited the range of observer angles at which noise was measured. For example, Devenport et al.⁶ measured the noise at 90° , and Moreau et al.¹⁰ considered observer angles ranging between 0° and 105° from the downstream direction. Thus it may be the case that previous measurements have been unable to capture the upstream behavior predicted in CAA studies.

Few authors have suggested reasons why leading edge noise is reduced for thick airfoils. While it has been shown that the surface pressure response is reduced by increasing airfoil thickness, it is not clear why this occurs. This paper aims to investigate the underlying mechanism behind the leading edge noise reduction for thick airfoils in order to better explain the noise reduction process.

III. Current work

The current work uses CAA methods to systematically study the effects on leading edge noise due to airfoil thickness t and leading edge radius R_{le} . Predictions are performed of the noise due to airfoils with varying t and R_{le} interacting with a single frequency harmonic gust to highlight the effects on noise due

to changes in both of these length-scale parameters. This study also assesses the validity of the flat plate assumption for modeling the leading edge noise of real airfoils. Noise predictions are made using accurate predictions of the non-uniform meanflow around the airfoil and again when the meanflow is assumed to be uniform everywhere, in order to assess the importance on noise predictions of accurate representation of the non-uniform flowfield. In addition to studying the noise reduction associated with real airfoil geometries, the current work also investigates the underlying mechanism which causes the noise reduction, so that the effects of airfoil geometry on noise can be better explained.

III.A. Airfoil geometry definition

For most airfoil families, such as the NACA 4-series airfoils, the leading edge radius R_{le} and the thickness t are related. For example, the NACA 4-series airfoils define $R_{le} \propto t^2$. If the thickness of a NACA 4-series airfoil is modified, therefore, there will be a corresponding change to R_{le} . Any effects on the leading edge noise will therefore be due to a combination of these two length-scale changes. In the current work, the effects on noise of R_{le} and t are investigated independently for the first time by using the NACA modified 4-series airfoil family¹⁵, which allow the separate specification of t and R_{le} . Leading edge radius R_{le} is related to thickness by

$$R_{le} = 0.5 \left[0.2969 \frac{t}{0.2} \left(\frac{I}{6} \right) \right]^2 \quad (1)$$

where I is a non-dimensional parameter which controls the shape of the leading edge as seen in Figure 2. $I = 0$ defines an airfoil with $R_{le} = 0$, while $I = 6$ represents a standard NACA 4-series profile. Through variations in I , the effects of leading edge radius changes with constant t can be studied.

The effects on leading edge noise are studied due to gust interactions with airfoils whose thickness varies between 6% (or $t = 0.06c$) and 24%, and whose I parameters vary between $I = 0$ and $I = 10$. An additional NACA 0002 case is also included for validation of the computational method, and is the closest approximation to a flat plate that is used in the CAA method. Figure 2 shows the geometries of the airfoils investigated. The naming convention follows the standard NACA 4-series method with an additional two digits which represent the parameter I and the chordwise position of maximum thickness (in tenths of chord) respectively. In this paper the chordwise position of maximum thickness is fixed at $0.3c$ and the airfoil chord is fixed at $c = 1$ m. This paper presents key results and trends observed from investigation of the noise from the various airfoils shown in Figure 2.

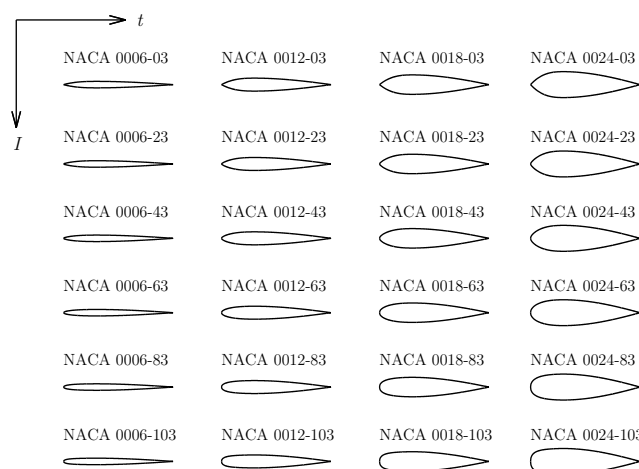


Figure 2. The various airfoil geometries used in the study. Both thickness and leading edge radius are varied to allow independent study of their effects on leading edge noise.

III.B. Modeling methods

The details of the analytic flat plate model and the CAA modeling strategy used in this paper are now discussed.

III.B.1. Analytic flat plate method

The flat plate analytic noise model due to Amiet⁴, modified to allow for 2D airfoils, is used for validation of the CAA method, and to assess the validity of using flat plate modeling for the prediction of real airfoil leading edge noise. The gust amplitude is taken to be constant at all frequencies, and set equal to $0.01U_x$ in both the analytic and CAA methods.

III.B.2. CAA method

The CAA method uses a high-order CAA code to solve the LEEs which has been used in previous aeroacoustic studies such as that by Zhang et al.¹⁶ A sixth-order compact spatial discretization scheme is used¹⁷ with tenth-order filtering and a fourth-order explicit temporal scheme¹⁸. Unsteady gusts are superimposed onto the steady meanflow solution which convects the vortical gust towards the airfoil. The effect on noise due to different steady meanflow solutions is investigated in this paper, and is discussed in Section IV.B. Far-field noise predictions are obtained from the airfoil surface pressure response and a Ffowcs-Williams and Hawkings (FW-H) solver which is based on Formulation 1A¹⁹.

Buffer conditions are used at all edges of the simulation to prevent spurious reflections from the domain edges interfering with simulation results. An explicit damping function is utilized at the end of each timestep²⁰ to damp perturbations to an assigned target value. The buffer zone transverse velocity target value is set equal to an unsteady value which defines the forced gust. This is done in order to prevent interactions between buffer zones and a separate gust boundary condition, and is similar to the method adopted by Kim et al.²¹.

One-dimensional vortical gusts with velocity component normal to the freestream direction are defined in this study to be of the form of a summation of discrete frequency gusts, and can be expressed as

$$w(x, T) = \sum_{i=1}^n w_o \cos(k_{g,i}[x - U_x T]) \quad (2)$$

where $w(x, T)$ is the instantaneous gust velocity, $k_{g,i}$ is the streamwise gust wavenumber of the i th frequency, x is the streamwise location, T is time, w_o is the maximum gust amplitude (set to $w_o = 0.01U_x$), and n is the total number of gust frequencies. Gusts at multiple discrete frequencies are defined in individual simulations, such that the vortical gust contains information at several discrete frequencies simultaneously. Sufficient numbers of frequency are chosen to resolve the spectral shape of the leading edge noise. Noise prediction at each discrete frequency is then recovered in post-processing via Fourier transformation.

C-shape grids are used near to the airfoil surface. Because of the differing grid requirements between viscous flow solutions and LEE propagation calculations, different computational grids are needed for the meanflow calculation and the gust interaction stages of the CAA method. Viscous computations are performed to obtain the steady meanflow solution where an accurate representation of the boundary layer is provided by using Y^+ values of below two. For the LEE simulations the resolution requirement is to resolve the forced gust. Therefore the LEE computational grid resolution is chosen to resolve the smallest gust wavelengths by at least 12 points per wavelength. Computational grids extend to 7 chord lengths from the airfoil in all directions to prevent acoustic interference with the domain edges. To allow acoustic gusts to be overlaid onto a viscous meanflow solution, the viscous flowfield is interpolated onto the acoustic grid.

IV. Results

IV.A. Validation

The CAA method was validated by comparing 2D analytic flat plate predictions at $M = 0.2$ with noise predictions from the CAA method due to a thin NACA 0002 airfoil ($I = 6, t = 0.02c$) in a uniform meanflow. The NACA 0002 airfoil is the closest approximation to a flat plate that has been tested. An exact flat plate was not investigated with the CAA method since spatial discretization errors in finite difference codes prevent the use of genuine flat plate geometry. These errors arise from difficulties in applying a boundary condition to the infinitely thin leading edge of the flat plate. A uniform meanflow was used in the CAA prediction for better comparison with the analytic solution, which also assumes a uniform meanflow.

The leading edge far-field noise at $r = 15m$ was predicted at reduced frequencies of between $K = 0.25$ and $K = 12.5$. Figure 3 compares the noise predictions from analytic flat plate theory with predictions from a NACA 0002 airfoil in the CAA method, where the NACA 0002 airfoil has been modeled by assuming a uniform and a viscous non-uniform meanflow. The CAA_{non-uniform} spectra and directivity shown in Figure 3 represent the CAA noise predictions in which viscous non-uniform meanflow effects around the NACA 0002 airfoil are included, and are discussed in Section IV.B.

Figure 3 shows agreement between the analytic and the CAA_{uniform} noise predictions of better than 1 dB at all tested gust frequencies and observer angles. The largest difference is seen in the directivity

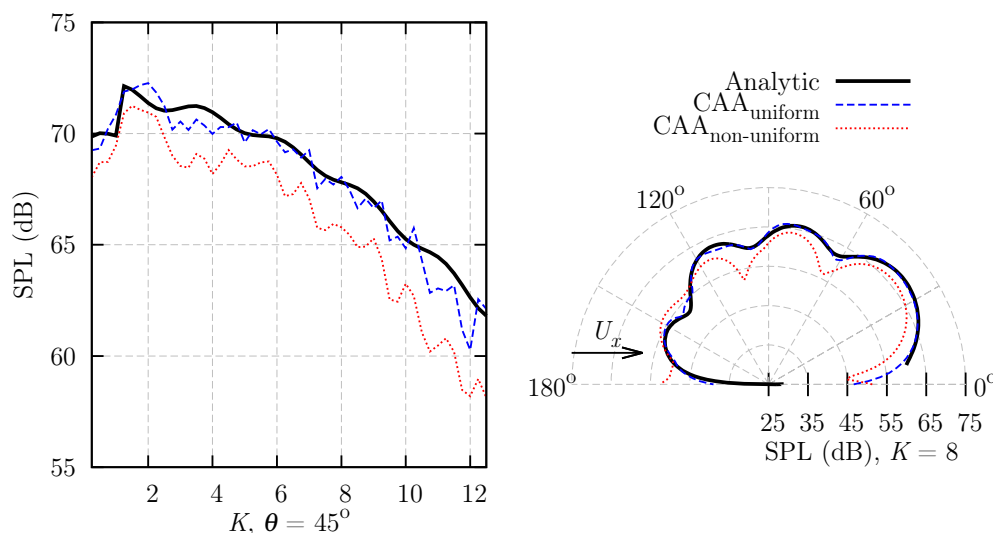


Figure 3. Spectral (left) and directivity (right) comparison of noise predictions from the CAA method using a NACA 0002 airfoil, and the analytic flat plate method. The spectral comparison is made at $\theta = 45^\circ$ and the directivity comparison is made at $K = 8$. CAA predictions using both a uniform and non-uniform flow are shown.

predictions at upstream observer angles, which can be attributed to the curvature of the NACA 0002 airfoil in the CAA method compared with a flat plate. Small oscillations in CAA spectral predictions can be seen. These are attributed to the assumption of discrete frequency forcing as opposed to a continuous spectrum, and to the fixed grid density, which causes each gust frequency to have a different temporal and spatial resolution in the simulation. The degree of agreement of better than 1 dB in Figure 3 provides validation of the CAA methods adopted in this paper.

IV.B. Meanflow modeling assumptions

We now investigate whether the modeling of the non-uniform meanflow is necessary for accurate noise prediction, or if accurate noise predictions can be obtained by making the assumption of uniform meanflow. This comparison also elucidates the noise generation mechanism, which is discussed in more detail in Section IV.E. Figure 3 compares the noise predictions made with the CAA method for a NACA 0002 airfoil, by using both the viscous non-uniform meanflow solution and by assuming a meanflow that is uniform everywhere. The non-uniform meanflow case predicts a lower noise amplitude of up to 3 dB at high frequency compared to the predictions made with a uniform meanflow and also to analytic noise predictions, at all frequencies and at most observer angles. The noise difference increases slightly with increasing frequency. Therefore, even with a thin NACA 0002 airfoil, the effects of a non-uniform meanflow are important to leading edge noise predictions. The effects of thickness on leading edge noise are discussed in further detail in Section IV.C.

Figure 4 shows the relative sound power level (PWL) predictions made using the analytic method, compared with predictions from the CAA method using a NACA 0012-63 airfoil at $M = 0.2, 0.4$, and 0.6 . Here, PWL is defined as the power per unit span for a 2D airfoil²². At each Mach number, noise predictions are made by the CAA method assuming a viscous non-uniform meanflow, an inviscid non-uniform meanflow, and a uniform meanflow, so that the effects on noise due to different meanflow assumptions can be investigated. The uniform meanflow and the inviscid non-uniform meanflow computed for $M = 0.2$ are shown in Figure 5.

Figure 4 shows that at all Mach numbers there is a significant difference of up to 5 dB between the CAA noise predictions that are made by assuming a uniform meanflow, and those made by including non-uniform meanflow effects. Predictions that include the effects of non-uniform meanflow show a reduction in noise due to the thickness of the NACA 0012-63 airfoil, whereas closer agreement was obtained for the NACA 0002

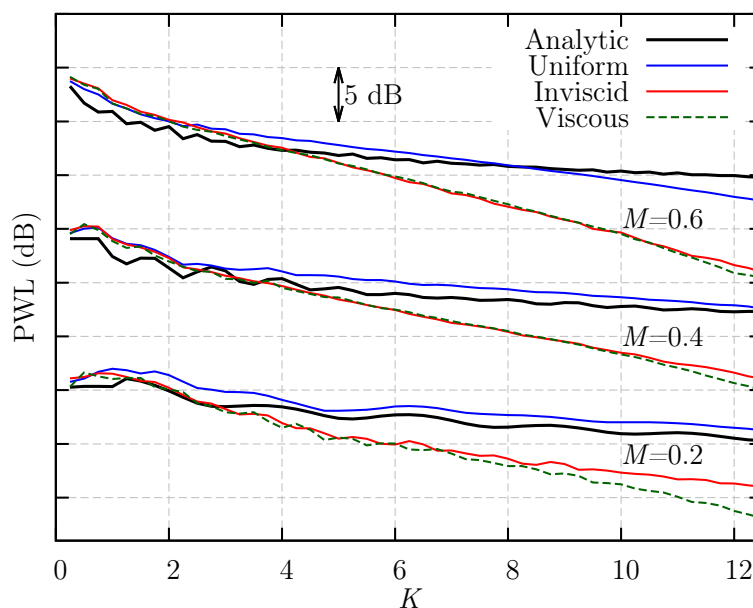


Figure 4. PWL due to harmonic sinusoidal gusts at varying reduced frequency interacting with a NACA 0012-63 airfoil. Predictions are made at $M = 0.2, 0.4$, and 0.6 by the analytic flat plate model and by the CAA method using differing meanflow assumptions.

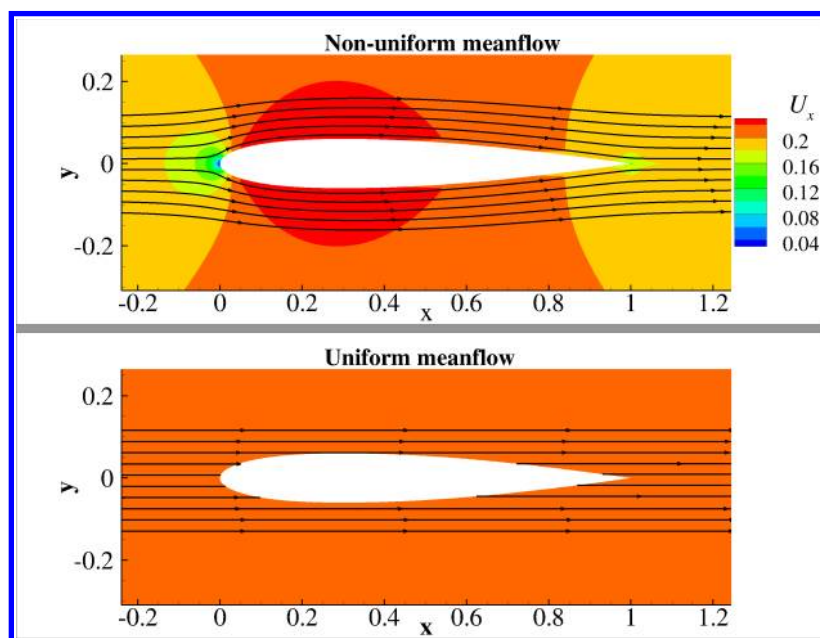


Figure 5. Comparison of an inviscid non-uniform and uniform meanflow result for a NACA 0012-63 airfoil at $M = 0.2$. Streamtraces outline flow direction and contours show U_x velocity.

airfoil in Figure 3. Therefore, it appears that the effect of the non-uniform meanflow at high frequencies is increased for airfoils with larger thickness. There is also a greater reduction in noise due to the non-uniform meanflow with increasing frequency and Mach number, which is in agreement with previous literature^{8,13}. At $K = 12$ and $M = 0.6$ the CAA predictions are approximately 9 dB lower than the predictions made with analytic flat plate theory. However, predictions that assume a uniform meanflow show an increase in noise in most cases. Therefore the non-uniform meanflow plays an important role in the leading edge noise generation mechanism of airfoils with real geometry.

Small differences of less than 1 dB are seen in the noise predicted by the CAA method between using a

viscous and inviscid non-uniform meanflow solution. Assuming an inviscid flowfield causes the CAA method to over-predict the noise by up to 1.5 dB at high frequency and low Mach number. In other parts of the spectrum the difference between the viscous and inviscid predictions is negligible. Therefore, for predictions of leading edge noise due to symmetric airfoils interacting with harmonic gusts, an inviscid flowfield can be assumed in most cases without significant loss of accuracy.

The error incurred by assuming a uniform meanflow with regards to leading edge noise prediction of real airfoils has not been previously investigated. Additionally, the small loss in prediction accuracy of up to 1.5 dB caused by the assumption of an inviscid flowfield has not been previously reported. The remainder of this paper sets $M = 0.2$ and assumes an inviscid non-uniform meanflow. Reasons for the inaccuracy of predictions made when assuming a uniform meanflow solution are discussed in Section IV.E.

IV.C. Effects of thickness

The sensitivity of leading edge noise to varying airfoil thickness is now investigated. Figure 6 compares the contours of SPL with varying observer angle θ and gust reduced frequency K , between the analytic flat plate noise predictions and predictions from the CAA method using a NACA 0024-03 airfoil. Two iso-lines of constant SPL are also shown in Figure 6 to assist comparison between the two analytic and CAA methods. A NACA 0024-03 airfoil has been chosen for the CAA prediction because it has a large thickness t and zero leading edge radius ($R_{le} = 0$), and therefore exhibits thickness effects on noise while minimizing any leading edge radius effects.

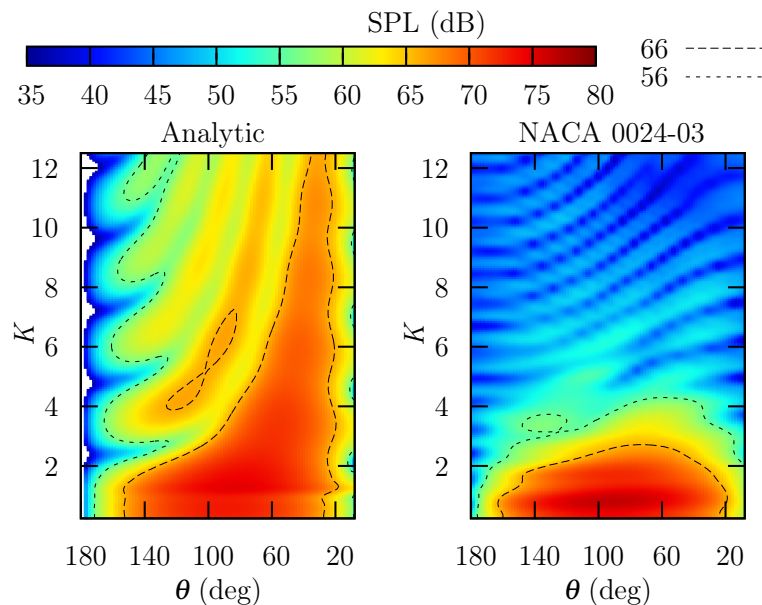


Figure 6. Comparison between the contours of SPL from analytic flat plate predictions (left) and the CAA method using a NACA 0024-03 airfoil (right), at varying observer angle and gust frequency.

Figure 6 shows that the noise predictions from the analytic and CAA methods give similar predictions at low frequency. However, at increasing reduced frequencies above $K = 1$ the CAA predictions are reduced in comparison to the analytic predictions, due to the thickness of the NACA 0024-03 airfoil. At $K = 12$ the NACA 0024-03 noise predictions are approximately 15 dB quieter than the flat plate predictions. Figure 6 shows that for downstream observers the effect of thickness on noise is significant for $K > 1$, which agrees with the conclusions of Atassi et al.¹³ but is lower than the conclusion of Paterson and Amiet⁷ that flat plate theory breaks down above about $K = 8.3$. At acute upstream angles ($170^\circ > \theta > 140^\circ$) the thickness of the NACA 0024-03 airfoil causes a less significant noise reduction.

The downstream lobe that is present at $\theta = 45^\circ$ in the flat plate prediction is not present in the CAA prediction for $K > 2$. As a result of this, the CAA predictions using the NACA 0024-03 airfoil exhibit less variation in noise amplitude with varying observer angle than is seen in flat plate predictions. The amplitude of the analytic flat plate noise prediction oscillates with varying frequency at forward observer

angles ($\theta > 140^\circ$). The CAA noise prediction also shows oscillations in noise amplitude with varying frequency above $K = 4$, but these oscillations are present over a wider range of angles compared with the analytic noise prediction.

Figure 7 compares the directivity predictions at $K = 8$ from the CAA method using airfoils with varying thickness, with those obtained from flat plate theory. Figure 7 shows that the directivity pattern remains similar as thickness is varied, but the predicted noise level reduces with increasing airfoil thickness at most observer angles. This finding agrees with the conclusions of several previous authors, including Olsen and Wagner⁸. However, at acute upstream observer angles between $170^\circ > \theta > 140^\circ$ the noise amplitude is not significantly reduced as a result of increasing thickness, as was also seen in Figure 6. At angles approaching $\theta = 180^\circ$ the noise for thick airfoils is increased in comparison with flat-plate analytic predictions. This is attributed to the presence of the rounded leading edge which will alter the orientation of the surface dipoles. Lockard and Morris¹⁴ and Atassi et al.¹³ both reported similar behavior to that shown in Figure 7, with the exception that both studies reported slight increases in upstream noise with increasing airfoil thickness. This increase is not seen in the current work.

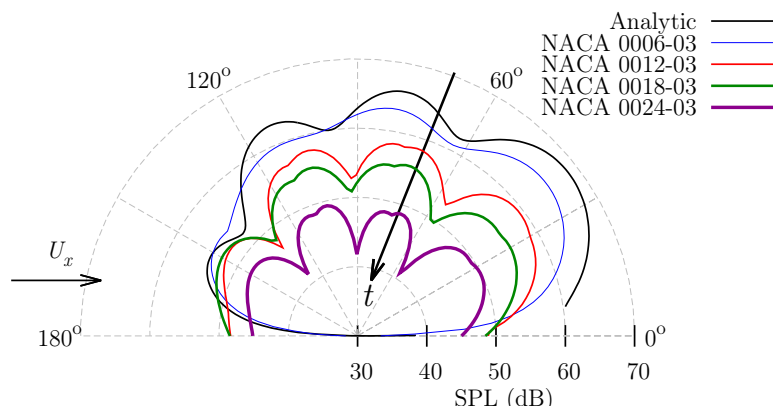


Figure 7. The effect on noise directivity predictions due to increasing airfoil thickness, with $R_{le} = 0$, at $K = 8$.

IV.D. Effects of leading edge radius

The effect of leading edge radius on leading edge noise is now investigated. Figure 8 shows the predicted leading edge noise spectra and directivity pattern due to a family of 12% thick airfoils with varying leading edge radii corresponding to $I = 0$, $I = 6$, and $I = 10$. Figure 8 shows that the predicted noise for downstream observers is reduced by increasing the leading edge radius, and that the amount of noise reduction increases with increasing reduced frequency. At upstream observer positions there is an increase in noise due to an increase in leading edge radius, but this trend is less clear than the trend for downstream observers since noise predictions for the NACA 0012-63 airfoil are greater than for the NACA 0012-10 airfoil. In general, the effect of increasing leading edge radius is to cause a reduction in noise for downstream observers, and to cause a slight increase in noise for upstream observers. Noise predictions become sensitive to leading edge radius at reduced frequencies above about $K = 4$, which is higher than the frequency of about $K = 1$ at which the noise appears to become affected by airfoil thickness.

We now investigate the relative sensitivity of the effects on noise due to thickness and leading edge radius. Figure 9 shows the PWL spectra for airfoils with 6% (or $t = 0.06c$) and 12% thickness, each with $I = 6$ and $I = 10$. At reduced frequencies above about $K = 1$, the noise predictions are significantly different between airfoils with differing thicknesses, with thicker airfoils generating less noise than thinner ones. Above reduced frequencies of about $K = 4$, the noise predictions for airfoils with equal thickness, but different leading edge radius, are reduced by an increase in the leading edge radius. Leading edge noise is therefore affected by airfoil thickness at lower reduced frequencies than it is affected by leading edge radius. Furthermore, the noise reduction due to the change from 6% to 12% thickness in Figure 9 is about 4 dB at $K = 12$, whereas the reduction in noise due to the change from $I = 6$ to $I = 10$ is about 2 dB at $K = 12$. Therefore leading edge noise appears to be more sensitive to the effects of airfoil thickness than to the effects of leading edge radius.

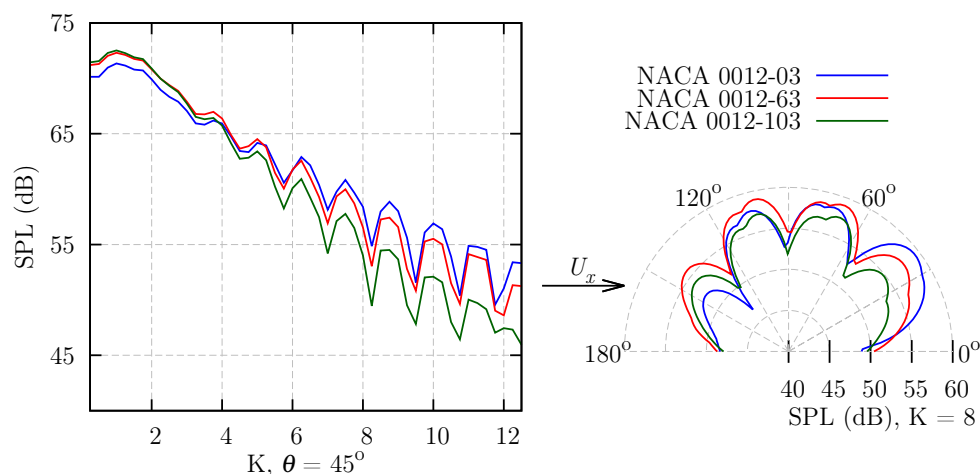


Figure 8. Spectral (left) and directivity (right) effects of the leading edge radius on noise from 12% thick airfoils. The spectral comparison is made at $\theta = 45^\circ$, and the directivity comparison is made at $K = 8$.

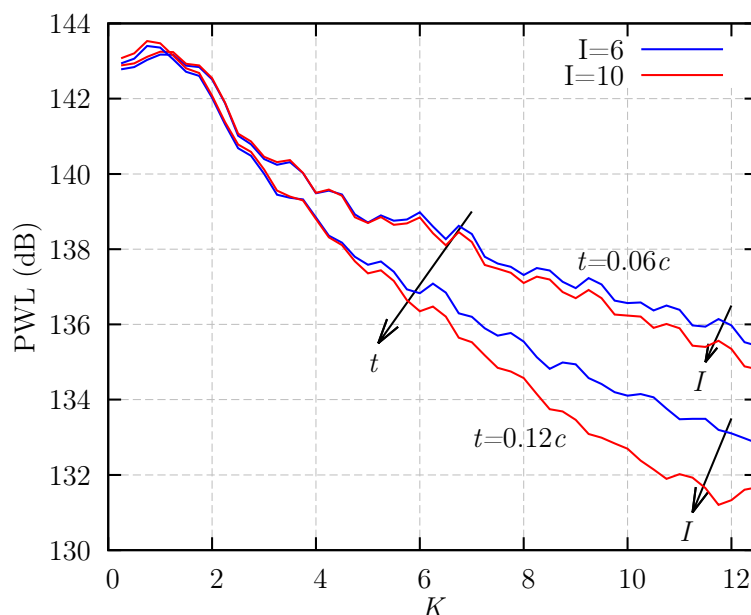


Figure 9. Comparison of the PWL behavior with chord-based reduced frequency, for airfoils with varying thickness and leading edge radius.

IV.E. Mechanism

This section investigates the mechanism underlying noise reductions due to increases in airfoil thickness and leading edge radius. Figure 10 shows the rms pressure p_{rms} along the surface of the front 20% of the airfoil chord, due to gust interactions at a reduced frequency of $K = 8$ with 2%, 6%, and 12% thick airfoils. Here, p_{rms} values have been normalized on the peak p_{rms} value of the NACA 0002 prediction. Figure 10 shows that as airfoil thickness is increased, the leading edge surface p_{rms} response is reduced, and also that the peak value of p_{rms} is moved downstream. This reduction in surface pressure response is the cause of the reduced far-field sound predictions in the CAA model, and agrees with the conclusions of Chiang and Fleeter¹¹ who used an analytic method to study the effects of thickness on the surface pressure response of an oscillating airfoil. However, the previous literature is not clear why the surface pressure response is reduced for airfoils with real thickness compared to flat plate predictions. The CAA method used in this paper allows this to be investigated by visualizing the unsteady flowfield surrounding the airfoil.

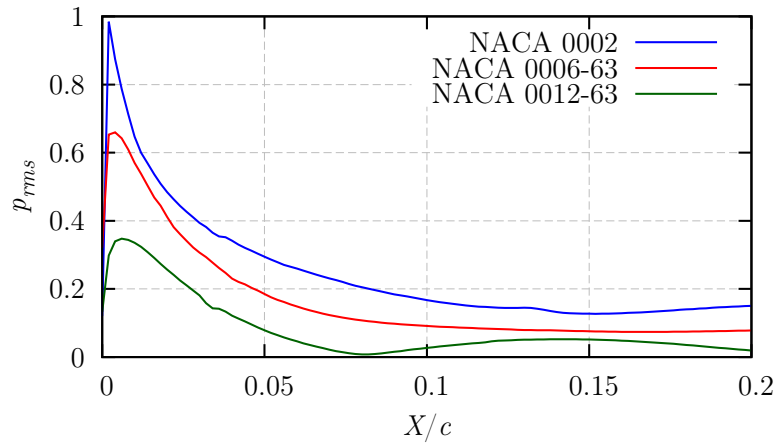


Figure 10. Normalized airfoil surface p_{rms} response due to a vortical gust at $K = 8$, for airfoils with $t = 0.02c$, $t = 0.06c$ and $t = 0.12c$.

Figure 11 shows a visualization of the instantaneous transverse velocity perturbations v for a high frequency vortical gust with $K = 8$, interacting with 2%, 6% and 12% thick airfoils. The solid lines show the shape of the gust wavefront, with arrows indicating the direction of the velocity perturbation. In this section v is non-dimensionalized by the speed of sound c_0 . Figure 11 shows that the gust wavefront is distorted by the real airfoil, and that this distortion increases with airfoil thickness. Distortion of the gust wavefront is caused by the velocity gradients present in the leading edge stagnation region, and is stronger for airfoils with larger thickness because thick airfoils generate a larger stagnation region. Figure 11 also shows that v is increased as the flow passes around the airfoil leading edge curvature. This effect is noticeable for all three airfoils shown in Figure 11, although it is less strong in the case of the NACA 0012-63 airfoil. This acceleration of the flow is caused by the induced circulation around the airfoil due to the gust. However, the increase in v around the leading edge is reduced when the gust wavefront is distorted by the leading edge stagnation region. Therefore, thick airfoils which cause a larger distortion of the gust wavefront will interact with reduced v values at the leading edge in comparison to thin airfoils. This reduction in v is therefore the main mechanism by which leading edge noise of real airfoils is reduced at high gust frequencies. This reduction in transverse perturbation velocity for thick airfoils is shown more clearly in Figure 12, which shows contours of time-averaged transverse velocity perturbations v_{rms} over one gust cycle for three airfoil thicknesses. Streamlines are also plotted in Figure 12 to show the path of the non-uniform meanflow around each airfoil.

Figure 13 shows contours of v for a low frequency vortical gust with $K = 1$, interacting with 2%, 6%, and 12% thick airfoils. Figure 13 shows that at low frequencies the airfoil thickness does not affect v . This is because the gust wavelength is large in comparison to the size of the stagnation region, so the gust wavefront is not significantly distorted by the velocity gradients.

In Figure 14 contours of v_{rms} are shown for a NACA 0012-63 airfoil interacting with a vortical gust at $K = 8$, when a uniform and a non-uniform meanflow is assumed in the CAA method. Figure 14 shows that when the meanflow is assumed to be uniform, v_{rms} values at the leading edge are greater in comparison to those modeled with a non-uniform meanflow. There is no stagnation region in a uniform meanflow, so the transverse velocity reduction mechanism discussed above is not included when a uniform meanflow is assumed. This explains the inaccurate noise predictions obtained when modeling leading edge noise of real airfoils interacting with vortical gusts using a uniform meanflow.

V. Conclusions

A CAA method has been applied to the modeling of leading edge noise due to harmonic vortical gusts interacting with various symmetric airfoil geometries at zero angle of attack. The effects of thickness and leading edge radius on the noise have been investigated, and the validity of flat plate analytic models has been assessed. The key findings of this paper are:

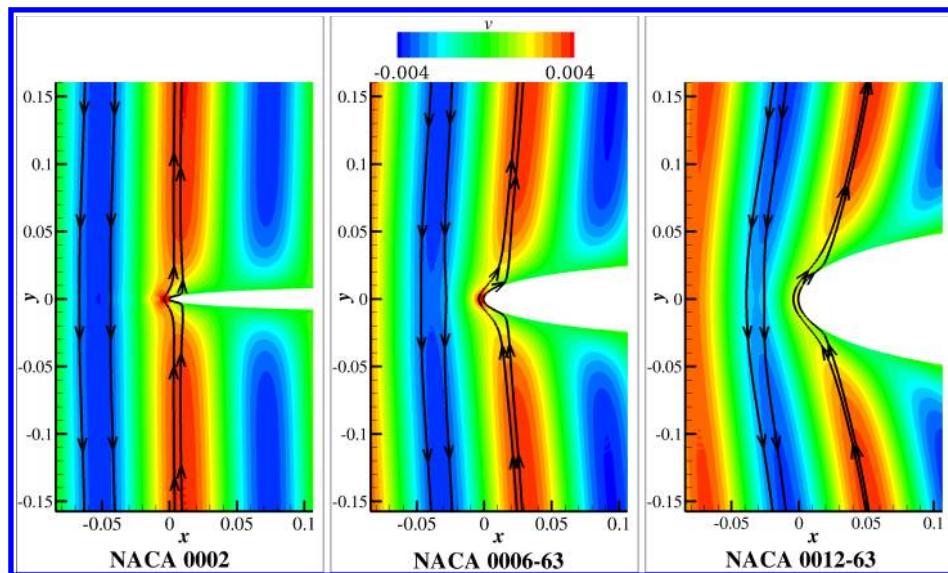


Figure 11. Contours of instantaneous transverse velocity perturbations v for a gust at $K = 8$ interacting with 2%, 6% and 12% thick airfoils. The solid lines represent the shape of the gust wavefront, with arrows showing the direction of the velocity perturbation.

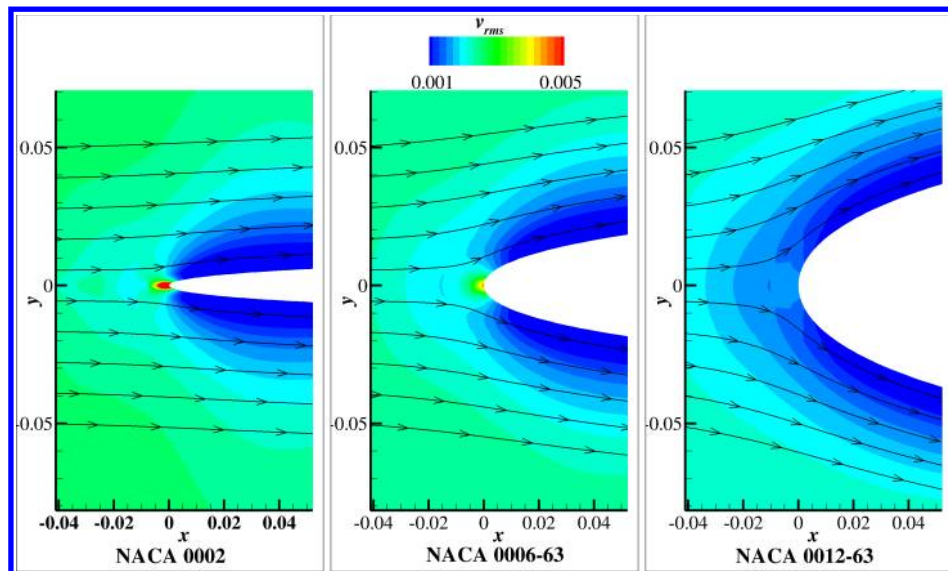


Figure 12. Contours of v_{rms} for a gust at $K = 8$ interacting with 2%, 6% and 12% thick airfoils. The contours are overlaid with streamlines of the non-uniform meanflow around each airfoil.

- The effect of increasing airfoil thickness is to reduce the leading edge noise in comparison to flat plate predictions, for reduced frequencies above about $K = 1$. The noise is reduced in the downstream observer direction more than it is reduced in the upstream observer direction. The noise reduction effect becomes stronger with increasing frequency, with increasing thickness, and with increasing Mach number.
- The effect of increasing leading edge radius is to reduce the noise at downstream observers and to increase the noise at upstream observers, in comparison to analytic flat plate predictions. The overall effect is to cause a reduction in PWL with increasing R_{le} . Leading edge noise becomes sensitive to leading edge radius changes for reduced frequencies above $K = 4$. However, leading edge noise is less sensitive to leading edge radius than it is to airfoil thickness.
- The effects of airfoil geometry on leading edge noise are noticeable even for 2% thick airfoils, such that analytic flat plate predictions will over-predict the noise from a NACA 0002 airfoil by approximately

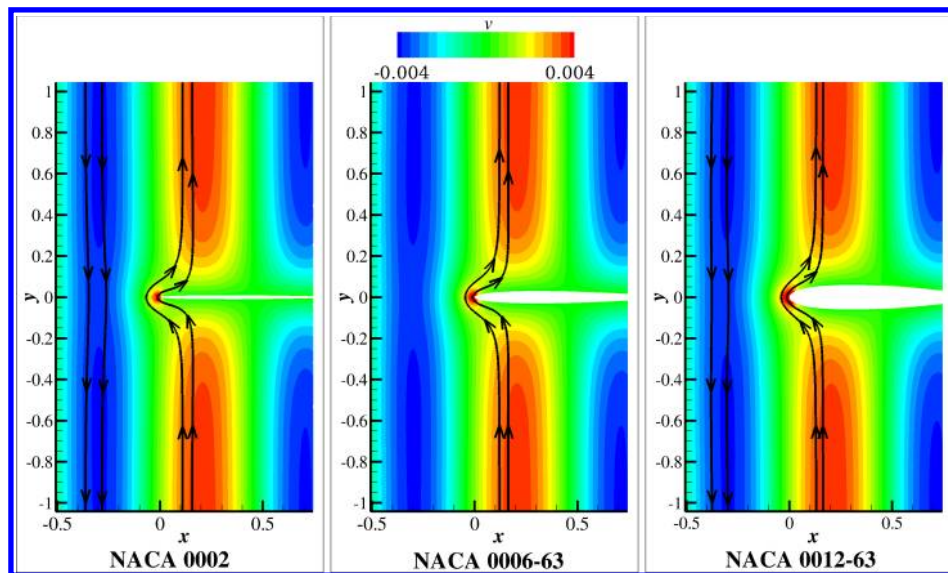


Figure 13. Contours of instantaneous transverse velocity perturbations v for a gust at $K = 1$ interacting with a NACA 0002, NACA 0006-63, and NACA 0012-63 airfoil. The solid lines represent the shape of the gust wavefront, with arrows showing the direction of the velocity perturbation.

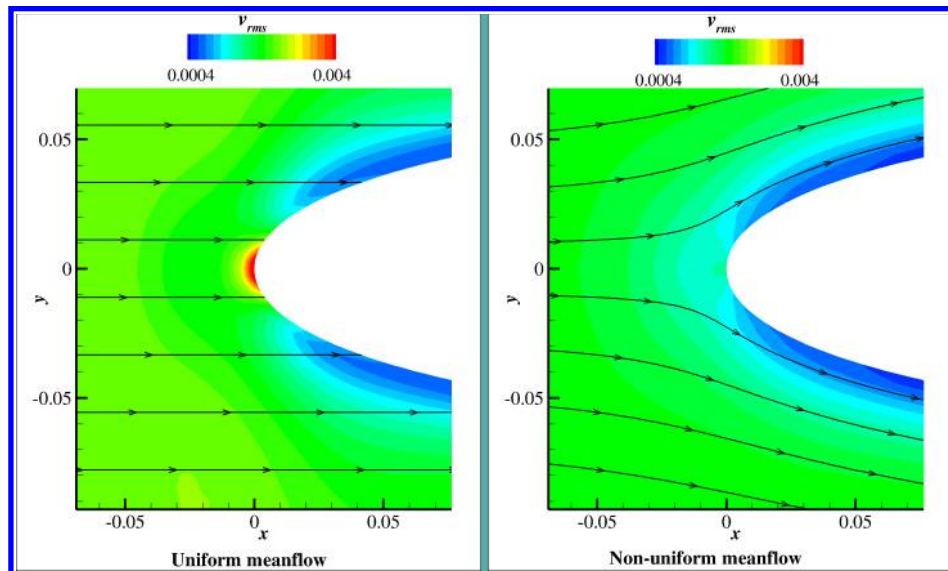


Figure 14. Contours of v_{rms} for a gust with $K = 8$ interacting with a NACA 0012-63 airfoil, modeled using a uniform and non-uniform meanflow. Streamlines are plotted to indicate the path of the steady meanflow field.

3 dB at high frequencies in $M = 0.2$ flow. For a NACA 0012-63 airfoil this over-prediction can be up to 9 dB at $K = 12$ and $M = 0.6$. The accuracy of flat plate analytic predictions of leading edge noise can be expected to decrease with increasing airfoil thickness, gust frequency and Mach number.

- The dominant mechanism that causes the discussed effects on noise, is related to the leading edge stagnation region. Vortical gusts are distorted by the velocity gradients in the stagnation region such that the wavefront of the gust across the leading edge is smoothed and the gust amplitude is reduced. Because the dominant noise reduction mechanism is associated with the meanflow, it is not valid to make an assumption of uniform meanflow when modeling the leading edge noise of airfoils with real geometry. However, an inviscid meanflow can be assumed without loss of prediction accuracy in most cases.

A limitation of the current work is that it only considers sinusoidal harmonic gusts at zero angle of attack. Extension of a CAA method to enable the modeling of broadband leading edge noise via synthesis

of a two-dimensional turbulent spectrum would provide interesting future study.

VI. Acknowledgment

The authors would like to thank the Industry Doctoral Training Center at the University of Southampton, the EPSRC, and Airbus for providing and funding the EngD project under which the current work is conducted.

References

- ¹“Flightpath 2050 Europe’s Vision for Aviation: Report of the High Level Group Research,” European Commission, 2011.
- ²Sears, W. J., “Some Aspects of Non-Stationary Airfoil Theory and its Practical Applications,” *Journal of Aerospace Sciences*, Vol. 8, 1941, pp. 104–108.
- ³Graham, J. M., “Similarity Rules for Thin Aerofoils in Non-Stationary Subsonic Flows,” *Journal of Fluid Mechanics*, Vol. 43, No. 4, 1970, pp. 753–766.
- ⁴Amiet, R. K., “Acoustic Radiation from an Airfoil in a Turbulent Stream,” *Journal of Sound and Vibration*, Vol. 41, No. 4, 1975, pp. 407–420.
- ⁵Staubs, J. K., Real Airfoil Effects on Leading Edge Noise, Ph.D. thesis, Virginia Polytechnic Institute and State University, 2008.
- ⁶Devenport, W. J., Staubs, J. K., and Glegg, S. A. L., “Sound Radiation from Real Airfoils in Turbulence,” *Journal of Sound and Vibration*, Vol. 329, 2010, pp. 3470–3483.
- ⁷Paterson, R. W. and Amiet, R. K., “Acoustic Radiation and Surface Pressure Response of an Airfoil due to Incident Turbulence,” Tech. Rep. CR-2733, NASA, 1976.
- ⁸Olsen, W. and Wagner, J., “Effect of Thickness on Airfoil Surface Noise,” *AIAA Journal*, Vol. 20, No. 3, 1981, pp. 437–439.
- ⁹Glegg, S. A. L. and Devenport, W. J., “Panel Methods for Airfoils in Turbulent Flow,” *Journal of Sound and Vibration*, Vol. 329, 2010, pp. 3709–3720.
- ¹⁰Moreau, S., Roger, M., and Jurdic, V., “Effect of Angle of Attack and Airfoil Shape on Turbulence Interaction Noise,” *11th AIAA/CEAS Aeroacoustics Conference, Monterey, California*, No. 2005-2973, 2005.
- ¹¹Chiang, H. D. and Fleeter, S., “Prediction of oscillating thick cambered aerofoil aerodynamics by a locally analytic method,” *International Journal of Numerical Methods in Fluids*, Vol. 8, 1988, pp. 913–931.
- ¹²Evers, I. and Peake, N., “On Sound Generation by the Interaction Between Turbulence and a Cascade of Airfoils with Non-Uniform Mean Flow,” *Journal of Fluid Mechanics*, Vol. 463, 2002, pp. 25–52.
- ¹³Atassi, H. M., Subramaniam, S., and Scott, J. R., “Acoustic Radiation from Lifting Airfoils in Compressible Subsonic Flow,” Tech. Rep. AIAA-90-3911, NASA, 1990.
- ¹⁴Lockard, D. and Morris, P., “Radiated Noise from Airfoils in Realistic Mean Flows,” *AIAA Journal*, Vol. 36, No. 6, 1998, pp. 907–914.
- ¹⁵Ladson, C., Brookes, C., Hill, A., and Sproles, D., “Computer Program to Obtain Ordinates for Naca Airfoils,” Tech. Rep. 4741, NASA, 1996.
- ¹⁶Zhang, X., Chen, X. X., and Nelson, P. A., “Computation of Spinning Modal Radiation from an Unflanged Duct,” *AIAA Journal*, Vol. 42, No. 6, 2004, pp. 1795–1801.
- ¹⁷Hixon, R., “Prefactored Small-Stencil Compact Schemes,” *Journal of Computational Physics*, Vol. 165, 2000, pp. 522–541.
- ¹⁸Hu, F., Hussaini, M. Y., and Manthey, J., “Low-Dissipation and Low-Dispersion Runge-Kutta Schemes for Computational Aeroacoustics,” *Journal of Computational Physics*, Vol. 124, No. 52, 1996, pp. 177–191.
- ¹⁹Farassat, F. and Succi, G. P., “The Prediction of Helicopter Rotor Discrete Frequency Noise,” *Vertica*, Vol. 7, No. 4, 1983, pp. 309–320.
- ²⁰Richards, R. K., Zhang, X., Chen, X. X., and Nelson, P. A., “The evaluation of non-reflecting boundary conditions for duct-acoustic computation,” *Journal of Sound and Vibration*, Vol. 270, 2004, pp. 539–557.
- ²¹Kim, J. W., Lau, A. S. H., and Sandham, N. D., “CAA Boundary Conditions for Airfoil Noise Due to High-Frequency Gusts,” *Periodica Engineering*, Vol. 6, No. 6, 2010, pp. 244–253.
- ²²Blandeau, V. and Joseph, P. F., “Broadband Noise Due to Rotor-Wake/Rotor Interaction in Contra-Rotating Open Rotors,” *AIAA Journal*, Vol. 48, 2010, pp. 2674–2686.